The International Society of Precision Agriculture presents the
15th International Conference on
Precision Agriculture
26–29 JUNE 2022
Minneapolis Marriott City Center | Minneapolis, Minnesota USA

The use of spatial and temporal indices to enhance the sensitivity of satellite-based spectral vegetation indices to water stress in maize fields

Yonatan Goldwasser[1,2], Victor Alchanati[1], Eitan Goldshtein[1], Guy Lidor[1], Ohaliav Keisar[1], Itamar Nadav[3], Ami Gips[3], Yafit Cohen[1].

[1] Institute of Agricultural Engineering, Agricultural Research Organization (Volcani institute), P.O. Box 15159, Rishon LeZion 7505101, Israel

[2] Institute of Plant Sciences and Genetics in Agriculture, The Robert H. Smith Faculty of Agriculture, Food & Environment, The Hebrew University of Jerusalem, Rehovot 76100, Israel

[3] Netafim, R&D Center, Derech Hashalom 10, Tel Aviv, Israel

A paper from the Proceedings of the
15th International Conference on Precision Agriculture
June 26-29, 2022
Minneapolis, Minnesota, United States

Abstract.

Currently estimating crop water requirements are achieved through the FAO-56 model. Models that rely on spectral vegetation indices (SVIs) derived from optical remote sensing became a reliable source of real-time crop coefficient estimations. While SVI-based crop coefficients (K_c) are more accurate in estimating plant water demands, they are less adequate for water status estimation. The goal of this study is to leverage satellite remote sensing data to determine Target Development Curves (TDCs) for the detection of unbalanced water status in maize fields. The first step to achieving this goal is to enhance the sensitivity of satellite based SVIs to water stress. Spectral, spatial, and temporal vegetation indices and their combinations based on Sentinel-2 images were generated for 215 commercial maize fields in Israel to identify indices with high sensitivity to stress that affected yield in early and peak growth periods. Average NDVI spectral time series grouped by yield levels showed that fields with low yield had lower NDVI values than those with high yield. Yet, the relative differences were low (8%), and they were observed around 30 days after sowing (DAS) with no differences in the peak period. The average angle at the near-infrared (ANIR) time series showed higher values for the low yield group with a relative difference of 18%. The spatio-spectral index, the NDVI-CV, i.e., its coefficient of variance (CV) was advantageous over the NDVI as the relative differences were higher (35%) and they were observed as early as 20 DAS. When a temporal index was added, i.e., the area under the curve of the NDVI-STD or ANIR-STD, differences were further enhanced and occurred also in the peak periods (60% and 35% at 20 and 65 DAS, respectively). Random forest (RF) for yield classification using the 30 most important indices obtained 0.67-0.82 overall accuracy for the calibration set for 4 time periods between 20-70 DAS. Additionally, the RF analysis has shown that combined indices or the temporal indices obtained the highest importance ranking and that the SWIR range was the most important in three selected DAS. The results show that a combination of spectral, spatial, and temporal indices may enhance the sensitivity of multi-spectral satellite images to water stress and may be used to further develop a library of TDCs based on them.

Keywords.

Spectral indices, Target Development Curves, Crop Water status, Irrigation.

1 Introduction

Water stress detection in fields is important to avoid yield loss and to promote optimal plant growth, yield quality, and yield stability. Climate change and water scarcity result in a challenge to find better ways for water management to increase irrigation water use efficiency (IWUE) thus, early water stress detection in fields is critical for field management and can aid policy-making for irrigation (Sagan et al., 2019). Presently, in extensive agricultural areas around the world, irrigation amounts are not estimated by direct measures of crop water requirement but by the ET_c FAO-56 model which provides guidelines for computing crop water requirements (Allen, 2000).

The model uses atmospheric evaporative demand together with calendar crop coefficients. Calendar crop coefficients may not adequately represent the actual phenological stage of a specific field in a specific year. Models that rely on spectral vegetation indices (SVIs) derived from optical remote sensing became a reliable source of so-called real-time crop coefficient estimation (Beeri et al., 2019; Kaplan et al., 2021; Rozenstein et al., 2018). These models are simple and easy to use but they suffer from several limitations. They assume normal crop development and thus do not account for plant water status which may lead to undesired positive feedback. With the aid of plant water status estimations, a water status coefficient can be added to the irrigation amounts thus overcoming these limitations. Over the past four decades, remote sensing of vegetation has focused on the optical-reflective range of the electromagnetic spectrum with multispectral sensors at the spaceborne level like Sentinel-2 (S-2) that offer different spatial and temporal resolutions of SVIs. Based on their indirect relationships to plant physiological and structural parameters such as canopy water content and fractional vegetation cover, SVIs are sensitive to a certain extent to plant water status. The spectral characteristics of water can be used to quantify the water content in the leaves. Short-wavelength infra-red (SWIR) bands and indices from multispectral airborne imagery were found to be correlated with plant water-related parameters and were important in estimating Fuel Moisture Content (FMC), Leaf Mass per Area (LMA), and Foliar Biomass (FB) (Casas et al., 2014). SVIs related to chlorophyll or leaf water content are related to late plant responses which tend to arise with visible symptoms hence their usage for pre-visual water-stress detection in crops is limited. SVIs reach saturation at peak growth stages and are not sensitive to further plant development. When reaching saturation, the monitoring of the plant is related to the identification of productive development and not the growth development. An alternative approach to detecting unbalanced water status is the use of Target Development Curves (TDCs). The TDCs serve as benchmarks for determining whether the crop is developing at an acceptable rate (i.e., on or off-target) and whether the crop is progressing towards maturity in an early and efficient manner (timing of physiological cutout). This research aims to leverage big remote satellite sensing data to determine TDCs for the detection of unbalanced water status in maize fields. This will allow us to extract water status coefficients and overcome the problems of the inability of assessing water stress at the peak growth stage due to the saturation of multispectral indices and the inability to assess stress before irreversible crop damage. The specific objectives of this study were: (a) to develop spatial and temporal indices as well as indices that combine spectral, spatial, and temporal features for early detection of plant water status-based S-2 images. (b) to build TDCs for *Zea mays L*. grown in Israel by selected remotely-sensed indices and (c) to examine whether combined indices based on spectral, spatial, and temporal have an advantage over the use of discrete spectral index values for the detection of canopy water stress in different growth stages and quantify it.

2 Methods

The general approach of this study was to use existing information about commercial fields and to identify fields with and without stress by their yield levels. Since no direct information about stress was available, the fields were grouped into three yield levels: high, medium, and low. The assumption is that the fields with high yield levels represent the best practice and their average SVI time series can be used to define TDCs, while fields with low yield levels represent fields that suffered from stress. Thus, indices that will show relatively high differences between fields with high and low yield levels will be adequate to be used for SVI-TDCs. The research methodology

workflow is presented in Figure 1.

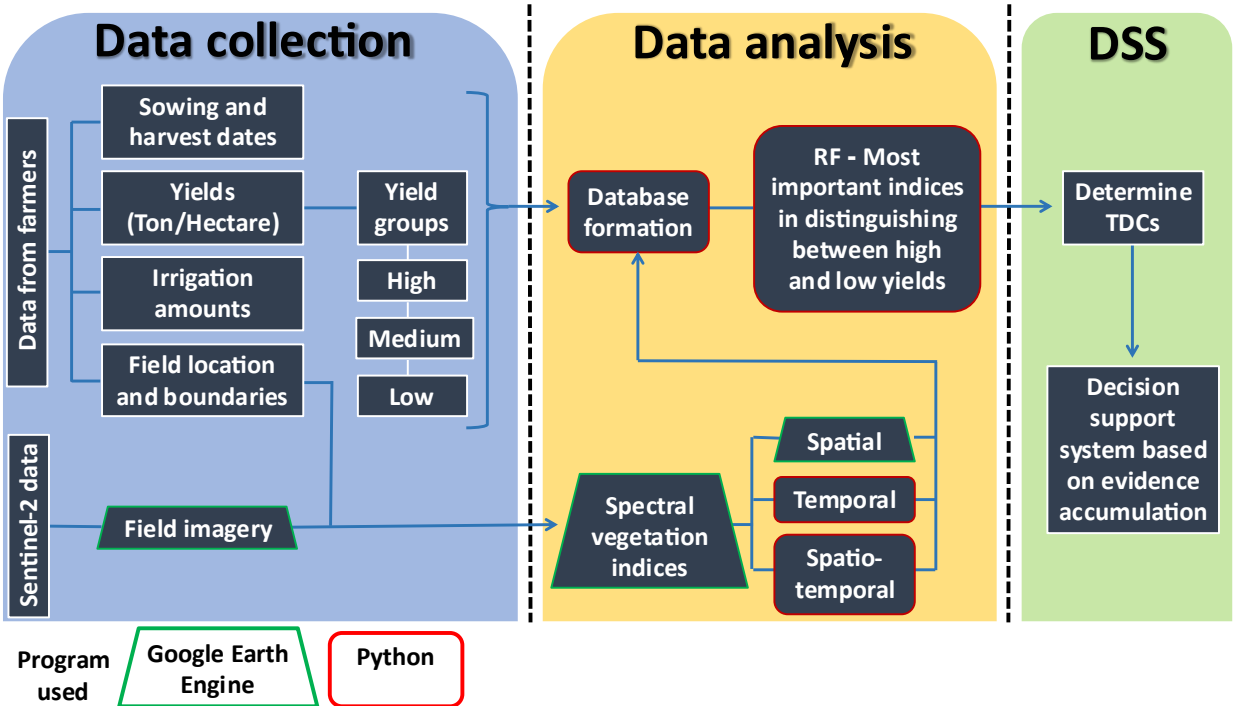

Fig 1 Research methodology workflow divided into 3 phases: a) data collection, b) data analysis, c) decision support system

2.1 Data sources and collections

2.1.1 Data collection from maize fields in Israel

Field data from 215 maize fields were collected from farmers in Israel during four growing seasons (2018- 2021) from the following farms: Tzora (31°46' N, 34°56' E), Tzabar Kama (31°45' N, 34°50' E), Yavne (31°46' N, 34°44' E), Bnei Darom (31°49' N, 34°42' E), Afek (32°50' N, 35°07' E), Heffer valley (32°22 N, 34°56' E) and Emek (32°38' N, 35°10' E). The data included field location and boundaries, maize species, agrotechnical operations, sowing and harvesting dates, irrigation amounts, and crop yields. QGIS software was used to create geographic layers of the fields that were uploaded as feature collections to the Google Earth Engine platform (GEE). The 215 field collection was split into three groups: the fields from 2019 (n=61) were used for qualitative comparison between indices by their ability to distinguish between fields with low and high yields; the 2018-2020 fields (n=163) were used to quantitively rank indices by their importance in distinguishing between fields with high and low yields and the 2021 fields (n=52) will be used later on for validation of the decision support system.

2.1.2 Satellite data

To monitor the collection of fields, spectral data of the crops was acquired by the S-2 mission that includes two identical multispectral satellites 2A and 2B which provide images of the earth with 5-day intervals. The satellite sensor includes 13 bands with 10 to 60m ground/spatial resolution covering visible, near-infra-red (NIR), and SWIR wavebands. Image collection for each field was obtained from the GEE platform according to the crop growing season in each area. GEE is a free cloud-based platform for geospatial analysis that stores many satellites imagery catalogs and geospatial datasets with planetary-scale analysis capabilities.

2.2 Data analysis

2.2.1 Satellite multispectral time-series for maize fields in Israel

From the S-2 images, time series of nine SVIs from different spectral ranges were calculated for each field along the growing season (Table 1). Using the sowing data received from the farmers each image date was transformed to days after sowing (DAS) to allow synchronization between phenological stages of the different fields.

Table 1. Spectral indices used to calculate Spatial and Temporal indices.

General Spectral range	Index	Formula	Sentinel-2 formula	Reference
* RGB	Visual atmospheric resistance index (VARI)	(Green - Red)/ (Green + Red - Blue)	(B3-B4)/(B3+B4-B2)	(Gitelson et al., 2002)
RGB	Green/Red Vegetation Index (GRVI)	(Green - Red)/(Green + Red)	(B3-B4)/(B3+B4)	(Tucker, 1979)
* Red edge	Red-Edge Inflection Point (REIP)	700 + 40 * (((Red + Red edge)/2)-Red edge) / (Red edge - Red edge)	700+40*(((B4+B7)/2)-B5)/(B6-B5)	(Guyot et al., 1988)
* Visual-NIR	Enhanced vegetation index (EVI)	2.5 * ((NIR - RED) / (NIR + 6 * RED - 7.5 * BLUE + 1))	2.5 * ((B8 - B4) / (B8 + 6 * B4 - 7.5 * B2 + 1))	(Huete et al., 2002)
* Visual-NIR	Normalized difference vegetation index (NDVI)	(NIR - Red) / (NIR + Red)	(B8-B4)/(B8+B4)	(Tucker, 1979)
Visual-NIR	Green Normalized Difference Vegetation Index (GNDVI)	(NIR – Green) / (NIR + Green)	(B8-B3)/(B8+B3)	(Gitelson & Merzlyak, 1996)
* SWIR and SWIR-NIR	The angle at near-infrared (ANIR)	$cos^{-1}[(a^2 + b^2 - c1^2) / 2 * a * b]$	$cos^{-1}[(a^2 + b^2 - c1^2)/2 * a * b]$	(Khanna et al., 2007)
SWIR and SWIR-NIR	Normalized Difference Water Index (NDWI)	(NIR – SWIR) / (NIR + SWIR)	(B8-B11)/(B8+B11)	(Gao, 1996)
* SWIR and SWIR-NIR	Shortwave angle slope index (SASI)	$\cos^{-1}[(a^2 + b^2 - c_2^2) / 2 * a * b] *$ [SWIR-NIR]	$\cos^{-1}[(a^2+b^2-c_2^2)/2*a*b]*$[B12-B8]	(Khanna et al., 2007)

* represents the indices left after filtering.

2.2.2 Enhanced SVIs

Based on the spectral data, spatial, temporal, and combined indices were calculated to exploit the spatial and temporal information in the satellite images and explore whether it can enhance the sensitivity of the satellite images to water stress. The spatial indices included: the standard deviation (STD) of the whole field, mean STD, and coefficient of variation (CV) of 3 by 3 kernels. The temporal indices included: slopes, the area under curves (AUC) between two images (ti and ti+1, and between ti and ti+2), and cumulative AUC. Finally, temporal indices were calculated on the spatial indices to produce spatio-temporal combined indices. In total 144 indices were produced for each field and were combined with the field data from the farmers to assemble a database that included all data collected on the fields. The calculation workflow of the indices is presented in Figure 2.

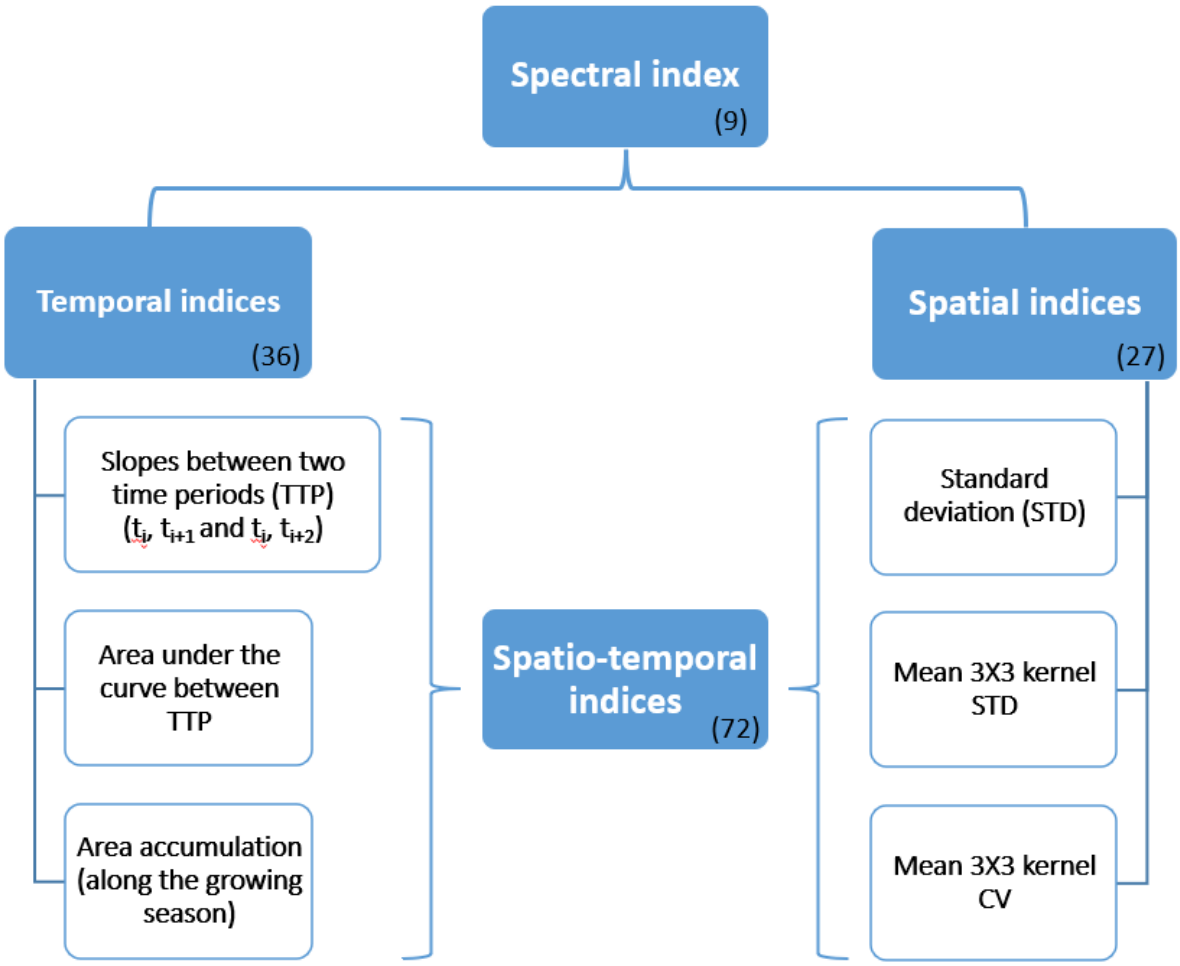

Fig 2 Spatial, temporal, and combined indices calculation flow chart. The number in the box indicates the number of indices that were calculated

2.2.3 Indices filtering and ranking

Index filtering was firstly performed to avoid co-linearity. The filtering was done by examining the correlations between indices in the overall database (all fields along the whole growing season). Wherever a linear correlation was obtained higher than r = 0.9, the selection for keeping an index was made by the index type and range according to the following priority (in descending order): SWIR range (because it is more directly related to water content), the Red Edge range, NIR, and Reed Green Blue (RGB) range. After the first filtering of the spectral type, spatial, temporal, and combined types were examined in the same process as the spectral type. The filtering process resulted in filtering three spectral indices which gave a total of 96 indices for each field. The six indices that were left after filtering are marked with an asterisk in Table 1.

The next step was to rank indices by their importance in distinguishing between fields with high and low yields. Random Forest (RF) classification was applied using all indices in four selected DAS from early to peak vegetative growth stages. RF classification outputs the importance of each index. For each selected DAS the 30 indices with the highest importance were selected for the second classification and the final ranking. Finally, the importance of the indices in each selected DAS was summed by index type (spectral, spatial, temporal, or combined) and spectral range (Table 1) to explore the relative contribution of each type and range.

3 Results and Discussion

Figure 3 shows the average Normalized difference vegetation index (NDVI) and the average angle at the near-infrared (ANIR) time series grouped by yield level along the growing season of 2019. On average, as expected, fields with low yield had lower NDVI values than those with high yield. Yet, they were observed only from 30 DAS and the relative differences were low (around 8%). Average ANIR time-series showed that fields with low yield had higher ANIR values than those with high yield, suggesting they had lower water content. Yet, they were observed only from 25 DAS and the relative differences were low (around 10%) which means they probably had lower water content levels. In both cases, the differences decrease in the peak growth stage apparently as a result of saturation.

Figure 4 shows the NDVI-CV and ANIR-CV time series grouped by yield levels along the growing season of 2019. In both cases, the spatial index shows enhanced differences in the early stages and sometimes in the growth peak stage. NDVI-CV shows that on average fields with low yields are associated with higher levels of variation. Relative differences of around 35% are noticeable in 20 and 65 DAS. This result is in accordance with the perception that a higher level of stress is associated with a higher level of variation. ANIR-CV shows differences of around 30% in 20 and 65 DAS but with a shifting trend that cannot be explained at this stage of the research.

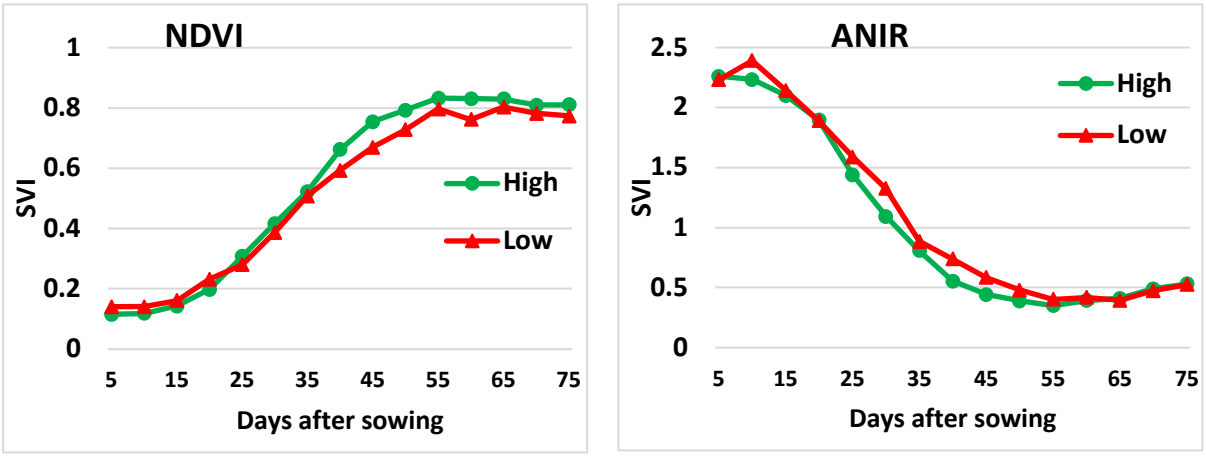

Fig 3 NDVI and ANIR 2019 fields averaged time-series grouped by yield level. The averages are based on all fields from 2019.

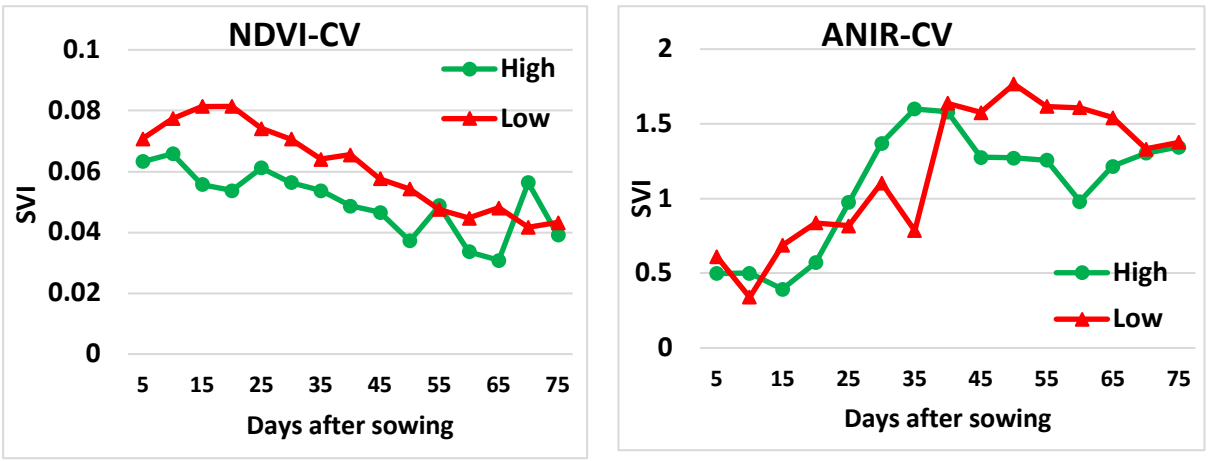

Fig 4 The average time-series of NDVI-CV and ANIR-CV grouped by yield level. The averages are based on all fields from 2019.

Figure 5 shows the AUC of the NDVI-STD and the AUC of the ANIR-STD time series grouped by yield levels along the growing season of 2019. When adding a temporal dimension to the spatial dimension (combined index), the differences are noticeable in both the early and peak growth stages. On average, fields with low yield had higher AUC-NDVI-STD values than those with high yield with a 60% relative difference at 20 DAS and 35% at 65 DAS. On average, fields with low yields had higher AUC-ANIR-STD values than those with high yields with a 58% relative difference at 20 DAS and 36% at 65 DAS. These results suggest that the spatial, temporal, and combined indices may enhance the sensitivity of multi-spectral satellite images to stress in maize fields as reflected by low and high yields.

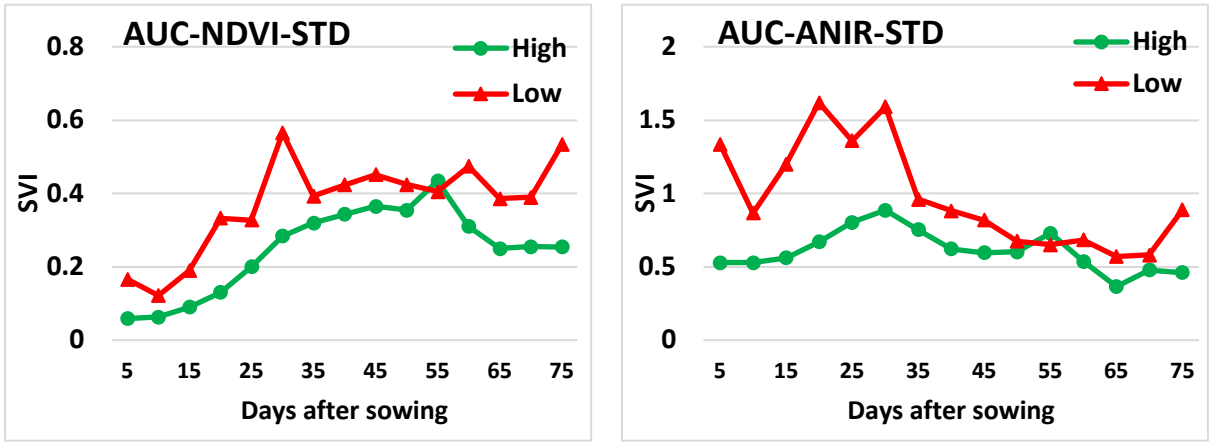

Fig 5 The average time-series of AUC-NDVI-STD and AUC-ANIR-STD grouped by yield level. The averages are based on all fields from 2019.

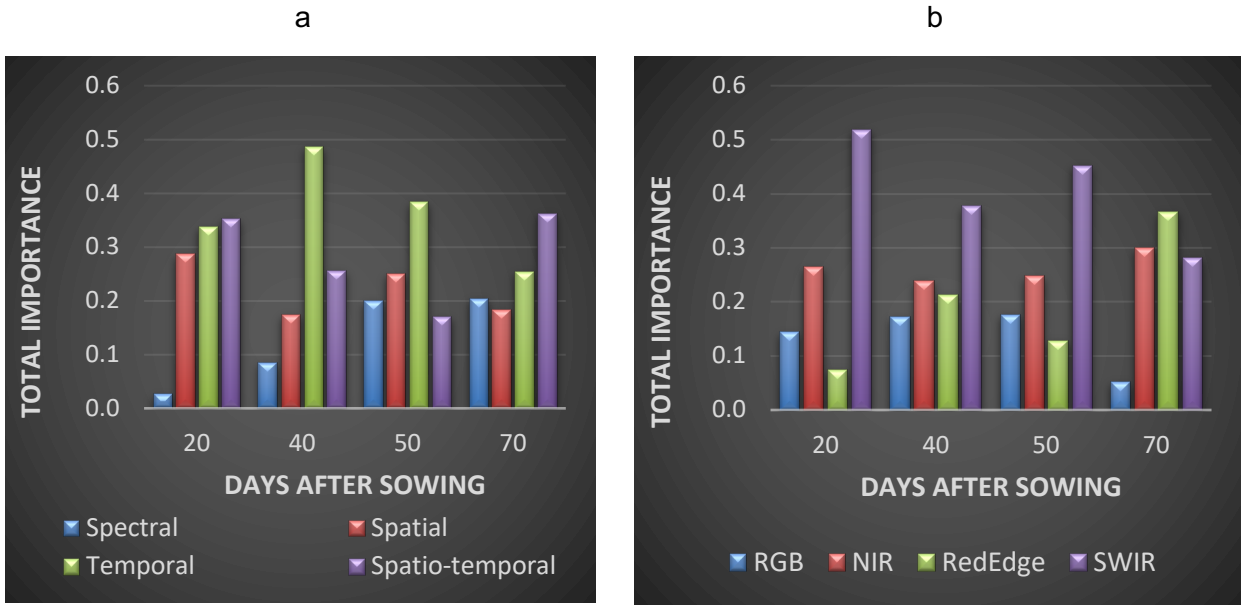

Fig 6 The summed importance of the 30 most important indices by index type (a) and spectral range (b) for each time period derived from a Random Forest classification.

Figure 6 shows the summarized importance of the 30 most important indices in distinguishing between high and low yield fields from 2018 to 2020 in each time period by index type and spectral range performed using the Random Forest algorithm. Among the types, there was no uniform

ranking trend in all selected DAS. Yet, the combined indices or the temporal indices obtained the highest ranking in 4 selected DAS. In relation to the spectral range, the ranking shows the SWIR obtained the highest ranking in 3 selected DAS while the RGB obtained the lowest ranking in 2 selected DAS. The RF classifications using the 30 most important indices obtained 0.67, 0.77, 0.75, and 0.82 accuracies for the calibration set at 20, 40, 50, and 70 DAS, respectively.

4 Conclusion

The results of this study showed that the sensitivity of satellite SVIs to water stress may be enhanced by spatial, temporal, and combined indices as reflected by low and high yields. Additionally, it seems that low yield levels are associated with water stress because of the high importance of the SWIR indices which are more directly related to water content. Further studies will define the SVI-TDCs based on the most important indices and integrate them into a decision support system. Based on every TDC, empirical thresholds will be determined for each growth stage. For the multiple TDCs approach, i.e. TDCs of other selected SVIs and spatial and temporal indices the Stanford Certainty Theory (Luger & Stubblefield, 1998; Cohen et al., 2008) will be utilized. This approach will allow us to accumulate certainties from various TDCs thresholds and to build a decision support system for field risk assessment that will be verified by the 2021 field data.

5 Acknowledgments

This research was supported by the Chief Scientist of the Israeli Ministry of Agriculture, Netafim, and the Israel Association of Field Crop Growers. We would like to thank the farmers for providing the information on the fields, the Netafim crew, and our colleagues from the Volcani institute for their time invested in helping the research.

6 References

Allen, R. G. (Ed.). (2000). *Crop evapotranspiration: Guidelines for computing crop water requirements* (repr). Food and Agriculture Organization of the United Nations.

Beeri, O., Pelta, R., Shilo, T., Mey-tal, S., & Tanny, J. (2019). *Accuracy of crop coefficient estimation methods based on satellite imagery* (p. 444). https://doi.org/10.3920/978-90-8686-888-9_54

Casas, A., Riaño, D., Ustin, S. L., Dennison, P., & Salas, J. (2014). Estimation of water-related biochemical and biophysical vegetation properties using multitemporal airborne hyperspectral data and its comparison to MODIS spectral response. *Remote Sensing of Environment*, *148*, 28–41. https://doi.org/10.1016/j.rse.2014.03.011

Cohen, Y., Cohen, A., Hetzroni, A., Alchanatis, V., Broday, D., Gazit, Y., & Timar, D. (2008). Spatial decision support system for Medfly control in citrus. *Computers and Electronics in Agriculture*, *62*(2), 107–117. https://doi.org/10.1016/j.compag.2007.12.005

Gao, B. (1996). Normalized difference water index for remote sensing of vegetation liquid water

from space. *Remote Sensing of Environment*, *58*(3), 257–266. https://doi.org/10.1016/S0034-4257(96)00067-3

Gitelson, A. A., Kaufman, Y. J., Stark, R., & Rundquist, D. (2002). Novel algorithms for remote estimation of vegetation fraction. *Remote Sensing of Environment*, *80*(1), 76–87. https://doi.org/10.1016/S0034-4257(01)00289-9

Gitelson, A. A., & Merzlyak, M. N. (1996). Signature analysis of leaf reflectance spectra: algorithm development for remote sensing of chlorophyll. *Journal of Plant Physiology*, *148*(3), 494–500. https://doi.org/10.1016/S0176-1617(96)80284-7

Guyot, G., Frederic, B., & Major, D. (1988). High spectral resolution: determination of spectral shifts between the red and the near infrared. *International Archives of Photogrammetry and Remote Sensing*, *11*, 750–760.

Huete, A., Didan, K., Miura, T., Rodriguez, E. P., Gao, X., & Ferreira, L. G. (2002). Overview of the radiometric and biophysical performance of the MODIS vegetation indices. *Remote Sensing of Environment*, *83*(1), 195–213. https://doi.org/10.1016/S0034-4257(02)00096-2

Kaplan, G., Fine, L., Lukyanov, V., Manivasagam, V. S., Malachy, N., Tanny, J., & Rozenstein, O. (2021). Estimating Processing Tomato Water Consumption, Leaf Area Index, and Height Using Sentinel-2 and VENμS Imagery. *Remote Sensing*, *13*(6), 1046. https://doi.org/10.3390/rs13061046

Khanna, S., Palacios-Orueta, A., Whiting, M. L., Ustin, S. L., Riaño, D., & Litago, J. (2007). Development of angle indexes for soil moisture estimation, dry matter detection and land-cover discrimination. *Remote Sensing of Environment*, *109*(2), 154–165. https://doi.org/10.1016/j.rse.2006.12.018

Luger, G., & Stubblefield, W. (1998). *Artificial Intelligence. Structures and Strategies for Complex Problem Solving. Addision Wesley Longman. Inc.,, 36, 39.*.

Rozenstein, O., Haymann, N., Kaplan, G., & Tanny, J. (2018). Estimating cotton water consumption using a time series of Sentinel-2 imagery. *Agricultural Water Management*, *207*, 44–52. https://doi.org/10.1016/j.agwat.2018.05.017

Sagan, V., Maimaitijiang, M., Sidike, P., Maimaitiyiming, M., Erkbol, H., Hartling, S., Peterson, K., Peterson, J., Burken, J., & Fritschi, F. (2019). UAV/satellite multiscale data fusion for crop monitoring and early stress detection. *International Archives of the Photogrammetry, Remote Sensing and Spatial Information Sciences - ISPRS Archives*. https://doi.org/10.5194/isprs-archives-XLII-2-W13-715-2019

Tucker, C. J. (1979). Red and photographic infrared linear combinations for monitoring vegetation. *Remote Sensing of Environment*, *8*(2), 127–150. https://doi.org/10.1016/0034-4257(79)90013-0